

3-2006

# Two-photon spectroscopy of rubidium using a grating-feedback diode laser

Abraham J. Olson

Evan J. Carlson

Shannon K. Mayer

University of Portland, mayers@up.edu

Follow this and additional works at: [http://pilotscholars.up.edu/phy\\_facpubs](http://pilotscholars.up.edu/phy_facpubs)



Part of the [Physics Commons](#)

---

## Citation: Pilot Scholars Version (Modified MLA Style)

Olson, Abraham J.; Carlson, Evan J.; and Mayer, Shannon K., "Two-photon spectroscopy of rubidium using a grating-feedback diode laser" (2006). *Physics Faculty Publications and Presentations*. 10.

[http://pilotscholars.up.edu/phy\\_facpubs/10](http://pilotscholars.up.edu/phy_facpubs/10)

This Journal Article is brought to you for free and open access by the Physics at Pilot Scholars. It has been accepted for inclusion in Physics Faculty Publications and Presentations by an authorized administrator of Pilot Scholars. For more information, please contact [library@up.edu](mailto:library@up.edu).

# Two-photon spectroscopy of rubidium using a grating-feedback diode laser

Abraham J. Olson, Evan J. Carlson, and Shannon K. Mayer

*Department of Chemistry and Physics, University of Portland, Portland, Oregon 97203*

(Received 29 July 2005; accepted 13 January 2006)

We describe an experiment for investigating the  $5S_{1/2} \rightarrow 5D_{5/2}$  two-photon transition in rubidium using a single grating-feedback diode laser operating at 778.1 nm (385 THz). Continuous tuning of the laser frequency over 4 GHz allows for the clear resolution of the Doppler-free spectral features and allows accurate measurement of the hyperfine ground-state splitting. A direct comparison between Doppler-broadened and Doppler-free spectral features is possible because both are distinctly evident in the two-photon spectra. By independently modifying the polarization state of the two laser fields, the impact of electric dipole selection rules on the two-photon transition spectra is investigated. This experiment is a valuable addition to the advanced undergraduate laboratory because it uses much of the same equipment as the single-photon saturated absorption spectroscopy experiment performed on the  $5S_{1/2} \rightarrow 5P_{3/2}$  transition in rubidium ( $\lambda=780.24$  nm) and provides students with an opportunity to investigate characteristics of atomic spectra not evident in the single-photon experiment. © 2006 American Association of Physics Teachers.  
[DOI: 10.1119/1.2173278]

## I. INTRODUCTION

Tunable diode lasers are used extensively in atomic physics research. In recent years grating-feedback diode laser systems have been developed that are suitable for construction by undergraduates.<sup>1-4</sup> These narrow-band (<1 MHz) laser sources provide several milliwatts of optical power (10–80 mW for the laser systems in Refs. 1–4) and have a typical frequency scanning range of 5–10 GHz.

Several atomic physics experiments have been developed for the advanced undergraduate laboratory to acquaint students with the basic techniques of laser spectroscopy and to investigate atomic properties. Recent atomic physics experiments that employ tunable diode lasers include the laser spectroscopy of rubidium and cesium,<sup>1</sup> the temperature dependence of Doppler-broadening in the absorption spectrum of rubidium,<sup>5</sup> atomic hyperfine structure studies in atoms,<sup>6</sup> observation of the Faraday effect using the  $D_2$  resonance line in a rubidium vapor,<sup>7</sup> and the laser spectroscopy of lithium<sup>8</sup> and the cesium dimer.<sup>9</sup>

Doppler-free saturated absorption spectroscopy of rubidium is among the simplest experiments using tunable diode lasers and the experiment is now widely used in the upper-division physics laboratory. The single-photon spectroscopy experiment employs a tunable diode laser tuned to the  $5S_{1/2} \rightarrow 5P_{3/2}$  transition ( $\lambda=780.24$  nm) in rubidium. Saturated absorption spectroscopy provides a valuable opportunity to observe the effect of Doppler broadening in atomic spectra and to investigate laser-saturation techniques for extracting the hyperfine structure features of the atomic system. A thorough description of saturated absorption spectroscopy can be found in Refs. 1 and 10. Reference 11 also reviews the relevant theory of Doppler-free saturated absorption spectroscopy and provides problems suitable for undergraduates.<sup>11</sup>

An investigation of the  $5S_{1/2} \rightarrow 5D_{5/2}$  two-photon transition in rubidium ( $\lambda=778.1$  nm) is a valuable complement to the single-photon spectroscopy experiment because it uses much of the same equipment, is conveniently accessible to a grating-feedback diode laser system designed for single-

photon spectroscopy at 780 nm, and offers the opportunity to directly resolve the hyperfine levels of rubidium without the presence of Doppler broadening. In addition, the experiment provides an opportunity for the direct investigation of the relation between laser light polarization, quantum mechanical selection rules, and the observed atomic spectra.

Two-photon transitions have historically been studied using stabilized tunable dye lasers and titanium sapphire lasers.<sup>12</sup> Subsequent observation of two-photon transitions in rubidium using AlGaAs diode lasers<sup>13,14</sup> make these experiments more accessible to undergraduates. Two-photon transitions in rubidium are of particular interest as new optical frequency standards due to their transition wavelength and narrow linewidth ( $\sim 300$  kHz linewidth for the two-photon transition).<sup>12</sup> Optical frequency references have fundamental and commercial applications, including uses in metrology, precision measurements, and the determination of fundamental constants. Precise frequency references in the near-infrared make enhanced studies of atomic spectra possible. Commercially, this rubidium two-photon transition is useful for optical communications work. Frequency stabilization of a frequency-doubled  $1.55 \mu\text{m}$  laser to the two-photon rubidium line provides a valuable frequency reference for the  $1.5 \mu\text{m}$  optical communications band.<sup>15,16</sup>

In this paper we describe the relevant theory for two-photon spectroscopy. We provide a detailed description of the experimental procedure and equipment, including references for commercial sources of equipment<sup>17</sup> and alternatives suitable for construction by undergraduates. We also give some typical experimental results and calculations that can be incorporated into the laboratory.

## II. THEORY

An energy level diagram of the relevant transitions in rubidium is shown in Fig. 1. The brightest spectral line, corresponding to the  $5S_{1/2} \rightarrow 5P_{3/2}$   $D_2$  line, has a transition wavelength of 780.24 nm (vacuum wavelength) and is often used for single-photon saturated absorption spectroscopy. The two-photon transition we investigated utilizes the  $5D_{5/2}$  ex-

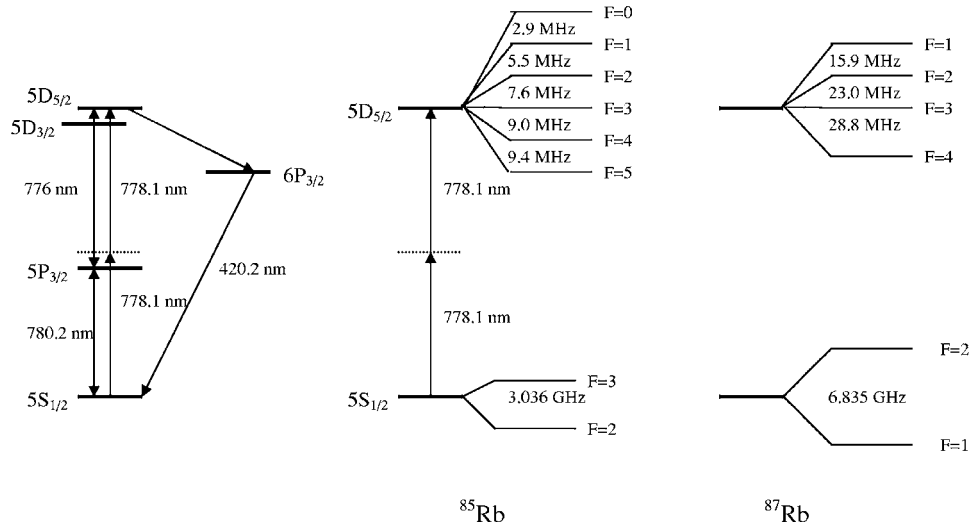


Fig. 1. Energy level diagram for rubidium. The relevant hyperfine levels for  $^{85}\text{Rb}$  and  $^{87}\text{Rb}$  are shown in the expanded view on the right-hand side. The  $5D_{5/2}$  hyperfine structure is inverted.

cited state, which is located 776 nm above the  $5P_{3/2}$  state. Two-photon absorption is achieved via the simultaneous absorption of two photons from a single laser tuned to 778.1 nm which excites the electron from the  $5S_{1/2}$  ground state to the  $5D_{5/2}$  excited state. Fluorescence can be monitored at 420 nm from the  $5D \rightarrow 6P \rightarrow 5S$  cascade decay. The expanded view to the right shows the relevant hyperfine structure for each of the rubidium isotopes.

The investigation of a two-photon transition typically requires a high-power laser. In this case the two-photon transition probability is greatly enhanced due to the proximity (2 nm detuning) of the near-resonant intermediate state.<sup>18</sup> The investigation of the  $5S_{1/2} \rightarrow 5D_{3/2}$  two-photon transition at 778.2 nm is also possible. However, the  $5S_{1/2} \rightarrow 5D_{5/2}$  transition is about 20 times stronger than the  $5S_{1/2} \rightarrow 5D_{3/2}$  transition due to the closer proximity of the intermediate state.<sup>12</sup> Two-step excitation to these  $5D_J$  states is also possible through the resonant intermediate state using two separate lasers at  $\lambda_1=780$  nm and  $\lambda_2=776$  nm.<sup>19</sup> Two-photon spectroscopy has also recently been performed using a diode laser on the  $5S_{1/2} \rightarrow 7S_{1/2}$  two-photon transition in rubidium ( $\lambda=760$  nm).<sup>20</sup>

The two-photon absorption process is illustrated in Fig. 2. Figure 2(a) shows an atom with velocity  $\vec{v}$  in the presence of two counterpropagating laser beams each tuned to the laser frequency  $\omega_L$ . For simplicity, we consider an atom moving collinearly with the laser beams, although the same result

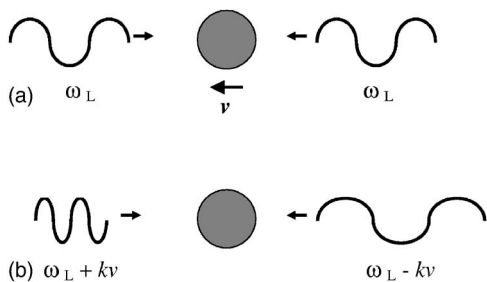


Fig. 2. (a) A moving atom between two counterpropagating laser beams. (b) Doppler-shifted laser frequencies as seen in the rest frame of the atom.

applies for a more general atomic trajectory. Due to the velocity of the atom, the laser frequency as seen in the rest frame of the atom [see Fig. 2(b)] is Doppler shifted by

$$\omega'_L = \omega_L \sqrt{\frac{1 \pm v/c}{1 \mp v/c}} = \omega_L - \vec{k} \cdot \vec{v} + \dots, \quad (1)$$

where  $k=2\pi/\lambda$ . To first order, the atom will “see” the laser beam from the left, Doppler shifted in frequency by an amount  $+kv$  while the laser beam from the right is shifted by an amount  $-kv$ . If the atom absorbs two photons simultaneously from oppositely directed beams, the two Doppler-shift terms cancel resulting in Doppler-free spectra, where all of the atoms contribute to the signal independently of their velocities. If the atom simultaneously absorbs two photons from the same direction, the Doppler-shift terms add together, resulting in a much weaker, Doppler-broadened signal.

The line shape of the Doppler-free portion of the two-photon spectra is Lorentzian and is given by<sup>18</sup>

$$L(\omega) \propto \frac{\gamma_{if}}{(\omega_{if} - \omega_1 - \omega_2)^2 + \frac{\gamma_{if}^2}{4}}, \quad (2)$$

where the transition frequency  $\omega_{if}$  between the initial and final state is  $2 \times (2\pi \times 385)$  THz and  $\omega_1 = \omega_2$  for two lasers with the same frequency. The full width at half-maximum intensity  $\gamma_{if}$  is the linewidth of the transition. The practical resolution of the linewidth is limited by the linewidth of the laser, which is larger in this case than the natural linewidth of the  $5S_{1/2} \rightarrow 5D_{5/2}$  two-photon transition.

The profile of a spectral line dominated by Doppler broadening is Gaussian and given by<sup>18</sup>

$$G(\omega) \propto e^{\{-4 \ln 2 [(\omega - \omega_0)^2 / \Delta\omega_{\text{Doppler}}^2]\}}, \quad (3)$$

and the Doppler-broadened linewidth is

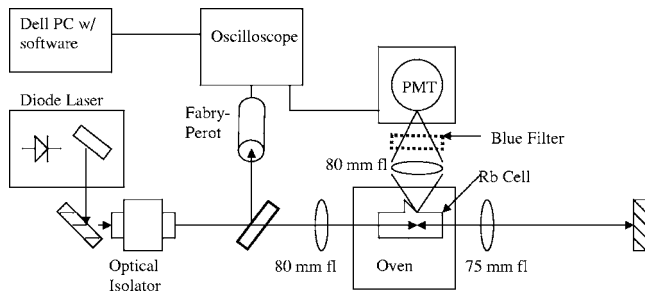


Fig. 3. Apparatus for the two-photon spectroscopy experiment.

$$\Delta\omega_{\text{Doppler}} = \frac{2\omega_0}{c} \sqrt{\frac{2k_B T}{m}} \ln 2, \quad (4)$$

where  $k_B$  is Boltzmann's constant,  $T$  is the absolute temperature, and  $m$  is the atomic mass.

Each of the rubidium isotopes have two hyperfine ground states ( $\sim$ GHz spacing) and several narrowly spaced hyperfine excited states ( $\sim$ MHz spacing). The four peaks corresponding to the different hyperfine ground states are easily resolved using a grating-feedback laser system with a 4 GHz scanning range. The ability to resolve the narrowly spaced hyperfine excited states may be limited by the linewidth of the laser system used and the quality of optical isolation available. The ratio of the intensities of the four hyperfine ground state peaks is determined by the statistical weights of the  $F$  states in the  $5S$  ground state.<sup>21</sup> For  $^{85}\text{Rb}$  the ratio of intensities of the  $F=3$  to the  $F=2$  line is 7:5. For  $^{87}\text{Rb}$  the ratio of intensities of the  $F=2$  to the  $F=1$  line is 5:3.

The observed spectra will also depend on the polarization state of the two laser fields. Single-photon optical transitions satisfy the selection rule  $\Delta L = \pm 1$  and therefore require ground and excited states of opposite parity, such as for the rubidium  $5S_{1/2} \rightarrow 5P_{3/2}$  transition. For two-photon transitions,  $\Delta L = 0$  or  $\Delta L = \pm 2$ , making  $S \rightarrow S$  and  $S \rightarrow D$  atomic transitions possible from the  $5S$  ground state in rubidium. For the  $5S_{1/2} \rightarrow 5D_{5/2}$  two-photon transition, the  $5D$  states can be reached when both beams have  $\sigma^+$  polarization. If one laser beam is polarized  $\sigma^+$  and the other is polarized  $\sigma^-$ , only  $S \rightarrow S$  transitions are possible because  $\Delta L = 0$ . The  $5S_{1/2} \rightarrow 5D_{5/2}$  two-photon transition also satisfies the selection rule that  $|\Delta F| \leq 2$ , thereby making possible transitions between many of the various  $F$  sublevels.

### III. EXPERIMENTAL APPARATUS

A diagram of the experimental apparatus is shown in Fig. 3. The laser system was a handbuilt, grating-feedback, extended-cavity diode laser operating in a Littrow configuration.<sup>2</sup> The laser diode is a Hitachi model HL 78516, specified to provide 50 mW of power at a typical free-running wavelength of 785 nm. The laser injection current was provided by a low-noise current control circuit.<sup>22</sup> Temperature stabilization of the diode was achieved using a proportional, integral, and differential feedback circuit<sup>23</sup> to regulate the current through a Peltier element located under the laser mount. The details for building a grating-feedback laser system are given in Refs. 1–4. Tunable diode lasers, current control circuits, and temperature control circuits with similar characteristics are commercially available.<sup>24</sup>

The output beam of the laser was directed through a rubidium vapor cell containing natural rubidium (72%  $^{85}\text{Rb}$ , 28%  $^{87}\text{Rb}$ ). The rubidium cell from Ophos Instruments was 100 mm long and 25 mm in diameter with optical quality windows. The temperature of the cell was controlled by a simple cylindrical oven that surrounds the cell. The oven was comprised of an aluminum tube wrapped with heat tape with holes to provide optical access for the laser beam and an exit path for the fluorescence signal. To prevent rubidium vapor from condensing on the cell windows, they were heated preferentially hotter than the center of the rubidium cell. The temperature of the tube was measured using a thermocouple temperature probe placed at the point in the oven closest to the imaged fluorescence region.

The laser power entering the rubidium cell was measured to be 16 mW. The laser was focused to a spot inside the cell using a pair of collimating lenses of focal length 75 and 80 mm. These values were selected based on the availability of lenses in our laboratory. Reflection from a plane mirror provided the counter-propagating laser beam. The two counterpropagating beams were carefully aligned to overlap in the rubidium cell. A ConOptics 712B optical isolator, rated at 30 dB isolation, was used to reduce unwanted optical feedback into the diode laser cavity.

The initial tuning of the laser to the two-photon transition wavelength was achieved by adjusting the position of the grating in the laser assembly and monitoring the output wavelength using a Burleigh WA-2500 Wavemeter<sub>r</sub> wavelength meter. A description of a simple, low-cost Michelson wavelength meter, suitable for construction and use in the undergraduate laboratory, is provided in Ref. 25. Current and temperature tuning of the diode provided further control of the output wavelength. Once the laser was at the desired wavelength, the cell was heated to a temperature of approximately 125 °C. At this point, fine adjustment and tuning of the output wavelength was provided by applying a voltage ramp to a piezoelectric transducer mounted behind the laser grating. The fluorescence signal was imaged onto a Burle 931A photomultiplier tube using an 80 mm focal length lens. A 420 nm interference filter reduced interference from scattered light. The photomultiplier tube signal was sent to an oscilloscope program on a personal computer, which exported the data to a spreadsheet for analysis. Blue fluorescence at 420 nm from the  $5D \rightarrow 6P \rightarrow 5S$  cascade decay was detectable at cell temperatures above 90 °C with 9.5 mW of laser power entering the rubidium cell.

To measure the hyperfine ground state splitting, the frequency of the grating-feedback diode laser was continuously scanned over 4.5 GHz by applying a linear voltage ramp to the laser grating piezoelectric transducer. To scan over the more narrowly spaced excited state hyperfine levels, the frequency scanning range of the laser was significantly decreased. Approximately 10% of the laser output was sent through a Thor Labs SA200-6A scanning Fabry-Perot interferometer with a 1.5 GHz free-spectral-range. The transmission peaks from the interferometer provided a frequency reference for characterizing the rubidium spectral features.

The polarization of the laser beams was controlled using a pair of quarter-wave plates. The output of the diode laser was nominally linearly polarized. To improve the linear polarization, a linear polarizer was placed after the optical isolator and aligned for maximum transmittance. Without the quarter-wave plates, both the incident and reflected laser beams were

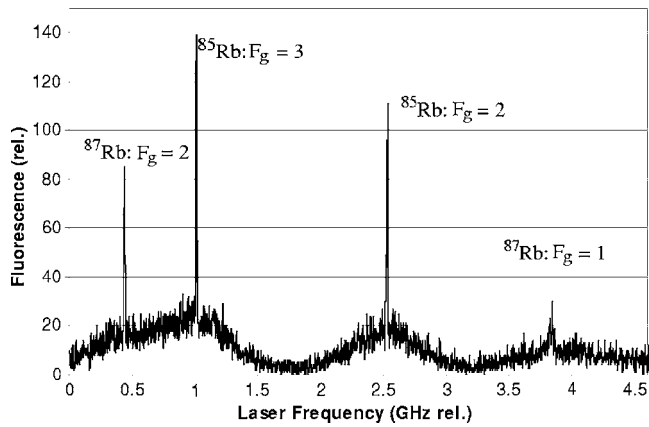


Fig. 4. Sample fluorescence spectrum of the  $5S_{1/2}-5D_{5/2}$  two-photon transition in rubidium. Note that the laser frequency spacing is one-half of the hyperfine ground state energy spacing for the two-photon transition.

linear polarized. By inserting one or both quarter-wave plates into the beam path, the incident and reflected beams could be polarized with the same or opposite circular polarization.

#### IV. EXPERIMENTAL RESULTS

Sample fluorescence spectra from the two-photon transition are shown in Fig. 4. The spectra show the measured fluorescence signal as the linearly polarized laser was scanned in frequency over a range of 4.5 GHz. Doppler-free peaks resulting from the four hyperfine ground states are clearly resolved. In addition, a weaker Doppler-broadened signal corresponding to two-photon absorption from a single beam is also evident. The ground-state hyperfine splitting was measured to be 3.05 GHz for  $^{85}\text{Rb}$  and 6.81 GHz for  $^{87}\text{Rb}$  with a measurement uncertainty of approximately 2% due to uncertainty in the frequency marker provided by the Fabry-Perot interferometer. These values are in excellent agreement with the published values of 3.036 GHz and 6.835 GHz for  $^{85}\text{Rb}$  and  $^{87}\text{Rb}$  respectively.<sup>12</sup>

The variation in peak heights from scan to scan was typically less than 10%. The peak height depended somewhat on the position of the spectral feature along the piezoelectric transducer voltage ramp. We monitored the laser output using the Fabry-Perot spectrometer and noticed that the laser approached mode instability near the end of the voltage ramp (the right-hand side of the data in Fig. 4). The mode instability corresponded to a variation in laser power, which affected the peak height. By adjusting the offset voltage to the laser piezoelectric transducer or by adjusting the diode temperature, the spectral features could be shifted to the right or the left relative to their position along the piezoelectric transducer voltage ramp. By shifting the peaks toward the left, we were unable to simultaneously scan over all four peaks. However, we did see an increase in the height of the  $^{87}\text{Rb}$   $F=1$  fluorescence peak by a factor of approximately 2 and a minor increase in the height of the  $^{85}\text{Rb}$   $F=2$  fluorescence peak. The frequency spacing between the peaks was independent of their relative position along the voltage ramp.

The ratios of the Doppler-free peak heights in Fig. 4 were measured to be approximately 11:9 for the two hyperfine ground states of  $^{85}\text{Rb}$  and approximately 11:4 for the two hyperfine ground states of  $^{87}\text{Rb}$ . These values differ from the predicted ratios of 7:5 and 5:3 for  $^{85}\text{Rb}$  and  $^{87}\text{Rb}$ ,

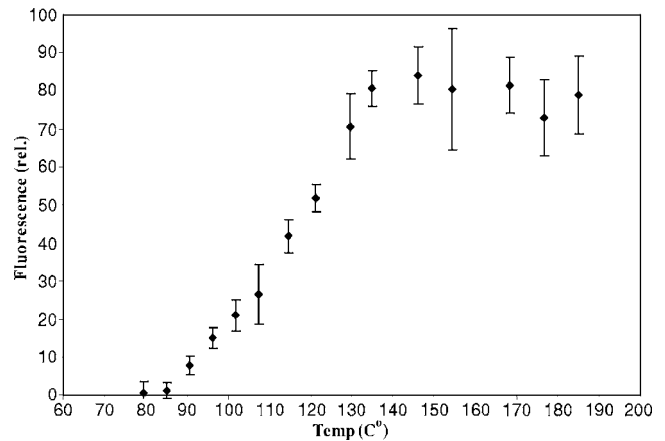


Fig. 5. The height of the  $^{85}\text{Rb}$   $F=3$  ground-state fluorescence peak is measured as a function of the temperature of the rubidium cell.

respectively.<sup>21</sup> When the peak heights were optimized independently (by adjusting the laser grating position or laser temperature), the measured values were found to be in much better agreement with the predicted ratios.

The relative height of the Doppler-broadened peaks compared to the Doppler-free peaks is accentuated in our data because the retro-reflected laser beam was misaligned slightly to reduce the optical feedback to the laser. Misalignment of the reflected beam significantly diminishes the intensity of the Doppler-free two-photon signal. The Doppler-broadened signal is much less affected because it arises from simultaneous absorption of two photons from the same beam.

The measured widths (full width at half-maximum) of the Doppler-free peaks in Fig. 4 were larger than the spread in the excited state hyperfine splitting—between 30 and 45 MHz—due to the linewidth of the laser and a slight frequency jitter caused by residual optical feedback. The Doppler-broadened peaks were fit using the Gaussian distribution given in Eq. (3). The measured linewidths were compared with the predicted Doppler-broadened linewidths from Eq. (4), calculated for our cell temperature, and found to be in very good agreement.

To aid students to find the fluorescence signal for the first time, the height of the  $^{85}\text{Rb}$   $F=3$  ground-state fluorescence peak was measured as a function of the temperature of the rubidium cell. The results are shown in Fig. 5 for an incident laser power of 9.5 mW. We observed an increase in the strength of the fluorescence signal over the temperature range from 90 °C to 130 °C. The signal size remained constant at temperatures above  $\sim 130$  °C. This result is in good agreement with the observations of Ryan *et al.* who reported that beyond 125 °C self-absorption of the  $6P_{3/2} \rightarrow 5S_{1/2}$  fluorescence negated an increase in signal.<sup>13</sup> We were also able to observe blue fluorescence with the naked eye at temperatures above 120 °C when 15 mW of laser power were sent through the rubidium cell.

If the optical isolator is removed, we found that the feedback into the laser caused instability in the laser output. Simultaneous scanning over the four ground-state peaks proved to be more challenging. We also observed greater fluctuations in the peak heights due to fluctuations in the output power of the laser. In addition, measurements of the spacing between the hyperfine ground-state peaks were less

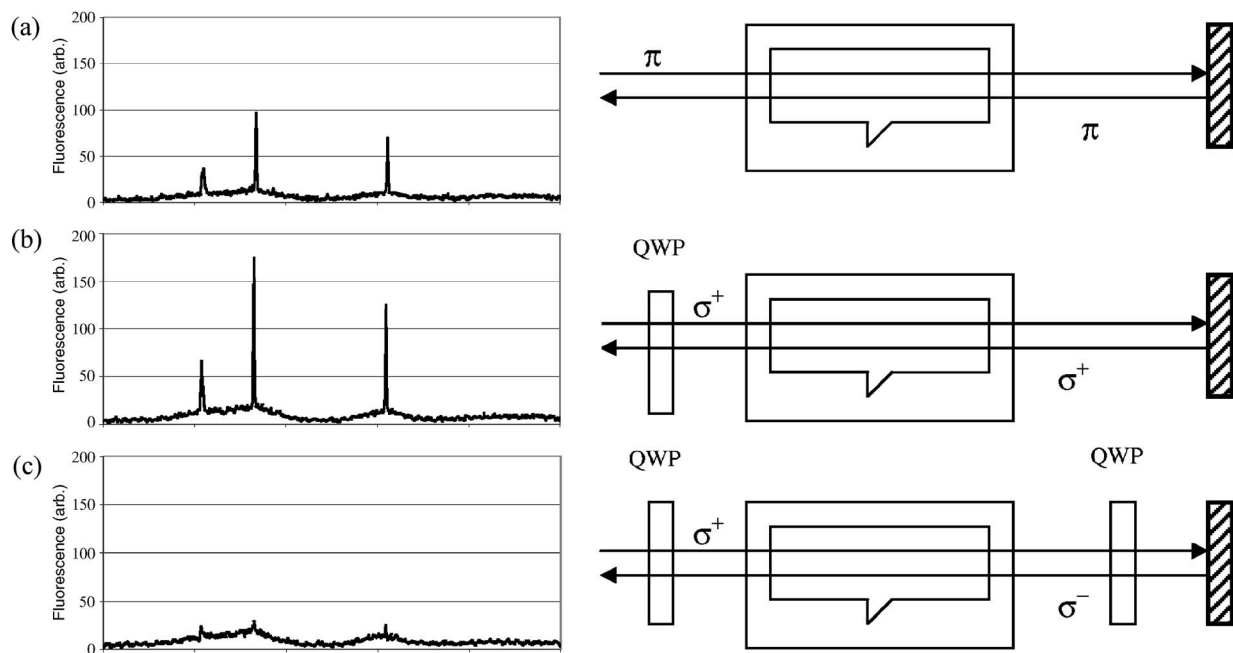


Fig. 6. The fluorescence spectra with (a) linear polarization, (b) circular polarization with each beam having the same polarization spin projection, (c) circular polarization with the incident and reflected beams having opposite polarization spin projection. The  $^{87}\text{Rb}$   $F=1$  peak is not evident in this data because of laser instability at the end of the scanning region during the collection of this data.

accurate because of spurious mode hops of the laser. With careful work we were able to scan over all four peaks by providing a linear voltage ramp to the laser piezoelectric transducer and manually adjusting the laser drive current. This approach does not give as accurate a measure of the hyperfine ground-state peaks spacing, but does give students an idea of both the approximate peak heights and the line shape of the Doppler-free and Doppler-broadened two-photon fluorescence spectra without the use of an optical isolator.

Figure 6 shows the effect of laser beam polarization on the two-photon signal. By inserting a single quarter-wave plate into the laser beam path before the rubidium cell and aligning it to produce circular polarization, both the incident and reflected laser beams have the same photon spin projection. This polarization configuration increased both the Doppler-free and Doppler-broadened fluorescence signals. When a second quarter-wave plate was inserted between the cell and the mirror, the circular polarization of the reflected beam was reversed, resulting in a theoretical loss of the Doppler-free signal ( $\Delta L=0$  in this configuration). Experimentally, we found the Doppler-free fluorescence signal to be nearly eliminated. The Doppler-broadened signal was not affected by the reversal in polarization of the return beam because both of the photons come from the same beam ( $\Delta L=2$ ). For  $S \rightarrow S$  transitions, such as the  $5S_{1/2} \rightarrow 7S_{1/2}$  two-photon transition in rubidium, this polarization configuration allows the Doppler-broadened signal to be eliminated, because  $\Delta L=2$  transitions are not allowed, while maintaining the Doppler-free spectral features.

The hyperfine excited states were studied by greatly reducing the frequency scanning range of the laser. We experimented with two methods; reducing the amplitude of the voltage ramp to the laser piezoelectric transducer and electronically scanning the laser current. We found current tuning of the laser provided better spectral resolution. A sample

fluorescence spectrum showing the hyperfine excited states is in Fig. 7. The expected results shown in Fig. 8 were constructed based on the high-resolution data obtained in Ref. 12. The experimental spectra were qualitatively similar to the spectral data in Ref. 12. The laser linewidth and instability due to optical feedback prevented clear resolution of the excited-state multiplets, except for  $^{87}\text{Rb}$   $F=2$ , for which the peaks are far enough apart to clearly resolve the individual peaks. We expect that an additional optical isolation stage would improve the resolution of the hyperfine excited states.

## V. SUMMARY

We have described a two-photon spectroscopy experiment using rubidium atoms that is suitable for an advanced undergraduate laboratory. By tuning a grating-feedback diode laser

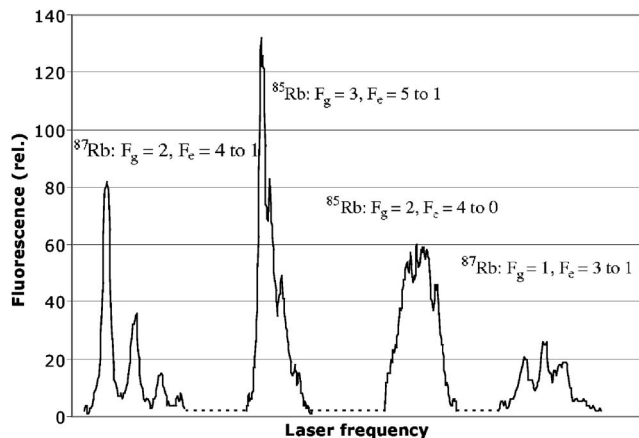


Fig. 7. Resolution of the hyperfine excited-state spectra for the four different hyperfine ground states.

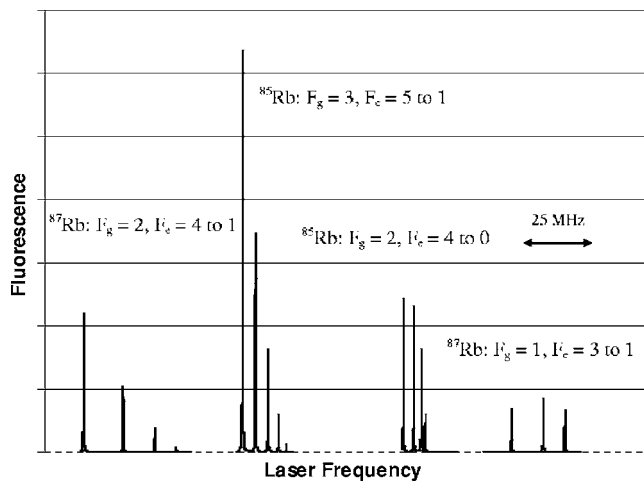


Fig. 8. The expected results for the hyperfine excited-state spectra constructed based on the high-resolution data obtained by Nez (Ref. 12). Note that the laser frequency spacing is one-half of the hyperfine excited state energy spacing for the two-photon transition.

operating at 778 nm over a 4 GHz frequency range, we obtained clearly resolved Doppler-free two-photon spectra that yielded accurate measurements of the hyperfine ground-state splitting in  $^{85}\text{Rb}$  and  $^{87}\text{Rb}$ . We compared Lorentzian and Gaussian spectral profiles for the Doppler-free and Doppler-broadened portions of the spectra, respectively, and investigated the impact of laser light polarization and quantum mechanical selection rules on the observed spectra.

## ACKNOWLEDGMENTS

The authors gratefully acknowledge the support of the M. J. Murdock Charitable Trust and the University of Portland. The authors would also like to thank Dr. John Essick of Reed College for the use of their optical isolator.

- <sup>1</sup>K. B. MacAdam, A. Steinbach, and C. Wieman, "A narrow-band tunable diode laser system with grating feedback, and a saturated absorption spectrometer for Cs and Rb," *Am. J. Phys.* **60**, 1098–1110 (1992).
- <sup>2</sup>J. J. Maki, N. S. Campbell, C. M. Grande, R. P. Knorpp, and D. H. McIntyre, "Stabilized diode-laser system with grating feedback and frequency-offset locking," *Opt. Commun.* **102**, 251–256 (1993).
- <sup>3</sup>A. S. Arnold, J. S. Wilson, and M. G. Boshier, "A simple extended-cavity diode laser," *Rev. Sci. Instrum.* **69**, 1236–1239 (1998).
- <sup>4</sup>R. S. Conroy, A. Carleton, A. Carruthers, B. D. Sinclair, C. F. Rae, and K. Dholakia, "A visible extended cavity diode laser for the undergraduate laboratory," *Am. J. Phys.* **68**, 925–931 (2000).
- <sup>5</sup>C. Leahy, J. T. Hastings, and P. M. Wilt, "Temperature dependence of Doppler-broadening in rubidium: An undergraduate experiment," *Am. J. Phys.* **65**, 367–371 (1997).

- <sup>6</sup>G. N. Rao, M. N. Reddy, and E. Hecht, "Atomic hyperfine structure studies using temperature/current tuning of diode lasers: An undergraduate experiment," *Am. J. Phys.* **66**, 702–712 (1998).
- <sup>7</sup>D. A. Van Baak, "Resonant Faraday rotation as a probe of atomic dispersion," *Am. J. Phys.* **64**, 724–735 (1996).
- <sup>8</sup>K. G. Libbrecht, R. A. Boyd, P. A. Willems, T. L. Gustavson, and D. K. Kim, "Teaching physics with 670 nm diode lasers-construction of stabilized lasers and lithium cells," *Am. J. Phys.* **63**, 729–737 (1995).
- <sup>9</sup>M. Terrell and M. F. Masters, "Laser spectroscopy of the cesium dimer as a physics laboratory experiment," *Am. J. Phys.* **64**, 1116–1120 (1996).
- <sup>10</sup>J. R. Brandenburger, *Lasers and Modern Optics in Undergraduate Physics* (Lawrence University Press, Appleton, WI, 1991), pp. 49–59.
- <sup>11</sup>D. W. Preston, "Doppler-free saturated absorption: Laser spectroscopy," *Am. J. Phys.* **64**, 1432–1436 (1996).
- <sup>12</sup>F. Nez, F. Biraben, R. Felder, and Y. Millerioux, "Optical frequency determination of the hyperfine components of the  $5S_{1/2}$ - $5D_{3/2}$  two-photon transitions in rubidium," *Opt. Commun.* **102**, 432–438 (1993).
- <sup>13</sup>R. E. Ryan, L. A. Westling, and H. J. Metcalf, "Two-photon spectroscopy in rubidium with a diode laser," *J. Opt. Soc. Am. B* **10**, 1643–1648 (1993).
- <sup>14</sup>Y. Millerioux, D. Touahri, L. Hilico, A. Clairon, R. Felder, F. Biraben, and B. de Beauvoir, "Towards an accurate frequency standard at  $\lambda = 778$  nm using a laser diode stabilized on a hyperfine component of the Doppler-free two-photon transitions in rubidium," *Opt. Commun.* **108**, 91–96 (1994).
- <sup>15</sup>M. Poulin, C. Latrasse, N. Cyr, and M. Tetu, "An absolute frequency reference at 192.6 THz (1556 nm) based on a two-photon absorption line of rubidium at 778 nm for WDM communication system," *IEEE Photonics Technol. Lett.* **9**, 1631–1633 (1997).
- <sup>16</sup>M. Zhu and R. W. Standridge, Jr. "Optical frequency standard for optical fiber communication based on the Rb  $5s$ - $5d$  two-photon transition," *Opt. Lett.* **22**, 730–732 (1997).
- <sup>17</sup>The identification of commercial suppliers and part numbers is given to provide thorough details. This identification is not intended as an endorsement or recommendation of these particular suppliers; alternate suppliers might provide similar equipment that meets or exceeds the performance of the equipment listed.
- <sup>18</sup>W. Demtroder, *Laser Spectroscopy*, 2nd ed. (Springer-Verlag, Berlin, 1996), pp. 466–473.
- <sup>19</sup>T. T. Grove, V. Sanchez-Villicana, B. C. Duncan, S. Maleki, and P. L. Gould, "Two-photon two-color diode laser spectroscopy of the Rb  $5D_{5/2}$  state," *Phys. Scr.* **52**, 271–276 (1995).
- <sup>20</sup>M. Ko and Y. Liu, "Observation of rubidium  $5S_{1/2}$ - $7S_{1/2}$  two-photon transitions with a diode laser," *Opt. Lett.* **29**, 1799–1801 (2004).
- <sup>21</sup>N. Bloembergen and M. D. Levenson, in *High-Resolution Laser Spectroscopy*, edited by K. Shimoda (Springer-Verlag, Berlin, 1976), Chap. 8, p. 355.
- <sup>22</sup>A. Hemmerich, D. H. McIntyre, D. Schropp, Jr., D. Meschede, and T. W. Hänsch, "Optically stabilized narrow linewidth semiconductor laser for high resolution spectroscopy," *Opt. Commun.* **75**, 118–122 (1990).
- <sup>23</sup>C. C. Bradley, J. Chen, and R. G. Hulet, "Instrumentation for stable operation of laser diodes," *Rev. Sci. Instrum.* **61**, 2097–2101 (1990).
- <sup>24</sup>Examples include New Focus tunable laser TLB-6312, Thor Labs tunable laser TL780-T, Thor Labs laser diode current controller LDC201U, and Thor Labs temperature controller TED200.
- <sup>25</sup>P. J. Fox, R. E. Scholten, M. R. Walkiewicz, and R. E. Drullinger, "A reliable, compact, and low-cost Michelson wavemeter for laser wavelength measurement," *Am. J. Phys.* **67**, 624–630 (1999).